© 2017. Published by The Company of Biologists Ltd | Journal of Experimental Biology (2017) 220, 2717-2725 doi:10.1242/jeb.158337

RESEARCH ARTICLE

Kinematics of ram filter feeding and beat–glide swimming in the northern anchovy *Engraulis mordax*

Nicholas Carey* and Jeremy A. Goldbogen

ABSTRACT

In the dense aquatic environment, the most adept swimmers are streamlined to reduce drag and increase the efficiency of locomotion. However, because they open their mouth to wide gape angles to deploy their filtering apparatus, ram filter feeders apparently switch between diametrically opposite swimming modes: highly efficient, streamlined 'beat–glide' swimming, and ram filter feeding, which has been hypothesized to be a high-cost feeding mode because of presumed increased drag. Ram filter-feeding forage fish are thought to play an important role in the flux of nutrients and energy in upwelling ecosystems; however, the biomechanics and energetics of this feeding mechanism remain poorly understood. We quantified the kinematics of an iconic forage fish, the northern anchovy, *Engraulis mordax*, during ram filter feeding and non-feeding, mouth-closed beat–glide swimming. Although many kinematic parameters between the two swimming modes were similar, we found that swimming speeds and tailbeat frequencies were significantly lower during ram feeding. Rather than maintain speed with the school, a speed which closely matches theoretical optimum filter-feeding speeds was consistently observed. Beat–glide swimming was characterized by high variability in all kinematic parameters, but variance in kinematic parameters was much lower during ram filter feeding. Under this mode, body kinematics are substantially modified, and *E. mordax* swims more slowly and with decreased lateral movement along the entire body, but most noticeably in the anterior. Our results suggest that hydrodynamic effects that come with deployment of the filtering anatomy may limit behavioral options during foraging and result in slower swimming speeds during ram filtration.

KEY WORDS: Swimming kinematics, Ram filter feeding, Forage fish, Anchovy

INTRODUCTION

The challenges of living in the dense, low-oxygen aquatic environment have driven the evolution of body plans and kinematic modes that minimize drag and increase the efficiency of locomotion. In fish, these adaptations are generally related to lifestyle and locomotor demands; highly mobile fish are generally streamlined, while benthic and sedentary species exhibit a wide range of body plans where minimizing drag may be less important than other habitat-specific adaptations, such as camouflage or maximizing prey capture success. Pelagic fish typically exhibit fusiform body forms and body–caudal fin propulsion mechanisms that increase the energetic efficiency of continuous or prolonged swimming. The scarcity and patchiness of food resources in the oceans has driven migration foraging strategies, and so the need to minimize the energetic costs of traveling large distances (Webb, 1984). Evolution of body plans that minimize drag has also been driven by the dynamics of targeting of schooling pelagic fish by high-speed predators such as tuna and sharks, along with whales and pinnipeds that exhibit search and chase foraging strategies (Blake, 2004; Domenici, 2003; Webb, 1984).

Forage fish, such as anchovies and sardines, form vast schools in areas of high primary productivity, thereby attracting large predator aggregations (Cury et al., 2000; Fleming et al., 2016). Their long migrations also drive the seasonal migrations of these associated predators (Gende and Sigler, 2006; Schweigert et al., 2010). Most forage fish are omnivorous, feeding primarily upon zooplankton and small pelagic invertebrates, and are an important intermediate link between lower and higher trophic levels in 'wasp-waist' pelagic food webs (Cury et al., 2000). Forage fish target prey of a range of sizes, and in doing so switch between distinct feeding modes; for smaller prey such as zooplankton, they filter feed; for larger prey, they bite to capture them, switching between these modes to maximize net energy intake (Crowder, 1985; Gibson and Ezzi, 1985, 1992). In anchovies, filter feeding is particularly energetically intensive (James and Probyn, 1989) because of the deployment of a wide filter-feeding apparatus. In this feeding mode, anchovies abandon streamlined swimming and swim with their mouth agape, driving water over the gill rakers to capture suspended prey (Fig. 1A). This ram filter feeding (RFF) is hypothesized to be a high-cost, high-intake physiological system that enables the rapid and bulk processing of the water column at the expense of increased drag and energy expenditure (Durbin et al., 1981; Macy et al., 1999; Sims, 1999, 2000). This is because the feeding structures of ram filter feeders typically present a high resistance to water flow (Sanderson and Wassersug, 1993).

With the pelagic realm lacking refuge, predation pressures have driven defensive schooling strategies in small pelagic fish. Schooling is important in energetic efficiency, lowering the mechanical costs of swimming via hydrodynamic effects (Herskin and Steffensen, 1998; Marras et al., 2015; Weihs and Webb, 1983) and through a 'calming effect' by reducing the need for individual vigilance (Nadler et al., 2016). Schooling can also protect against predation by confusing or intimidating predators (Handegard et al., 2012; Ioannou et al., 2012; Rieucau et al., 2014). Many predator strategies involve separating individuals or small groups to make them easier to capture (Domenici et al., 2014; Herbert-Read et al., 2016; Neill and Cullen, 1974). Thus, school integrity is important in minimizing collective energetic costs and, individually, in reducing predation risk. Any factor that reduces the cohesion of the school, such as a reduction in individual swimming speed, may cause

Hopkins Marine Station, Stanford University, 120 Ocean View Boulevard, Pacific Grove, CA 93950, USA.

*Author for correspondence (ncarey@stanford.edu)

N.C., 0000-0001-6715-8230

Received 15 February 2017; Accepted 8 May 2017

Journal of Experimental Biology (2017) 220, 2717-2725 doi:10.1242/jeb.158337

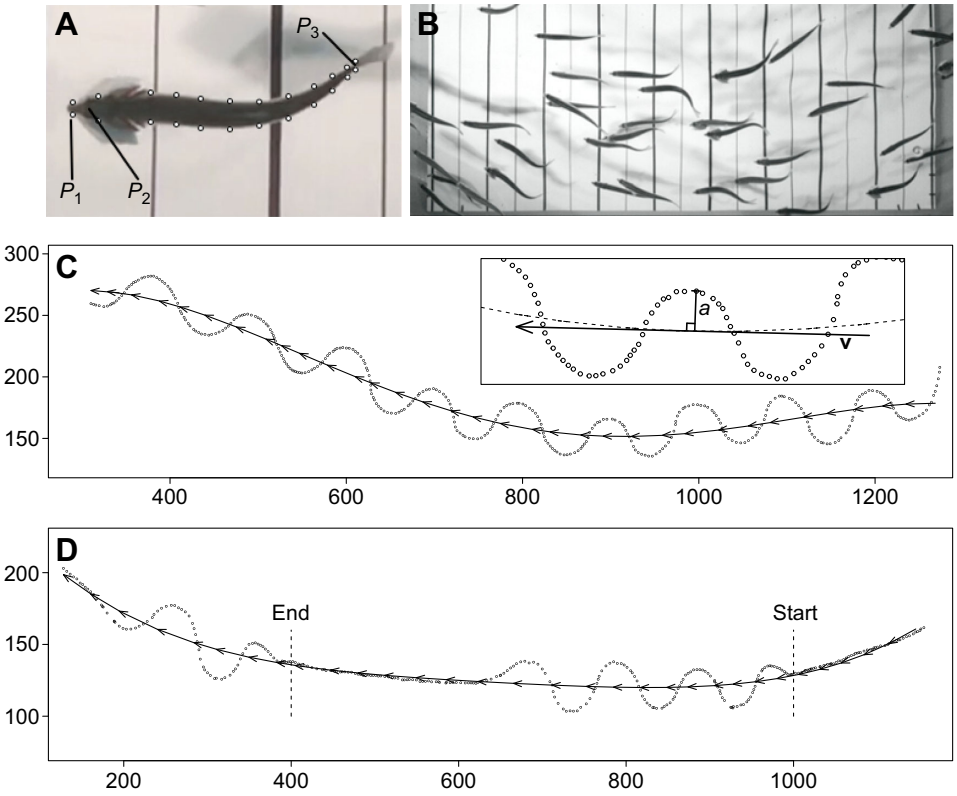

Fig. 1. Experimental procedure. (A) Points digitized for each specimen. Swimming kinematics: P_1, nose; P_2, midpoint between eyes; P_3, base of caudal fin. White circles indicate points digitized for midline kinematics (not all shown). (B) Screenshot from captured video. (C) Tail kinematics of ram filter feeding (RFF). *x*- and *y*-axes indicate spatial coordinates in pixels of the captured video at 13 pixels cm^{-1}. The solid line denotes a 4th order polynomial regression through tail coordinates describing the path across the arena, with arrows denoting the direction vectors (**v**) (see Materials and methods; only every 10th **v** is shown for clarity). The inset shows how tailbeat amplitude (*A*) was determined. *a* denotes the perpendicular distance to **v**, here shown extended for clarity. Tailbeat amplitude was calculated as the sum of adjacent maximum *a* values for each left and right tail extent. *A* was calculated as the average of these for all full strokes captured in the sequence. (D) A similar plot for beat–glide (BG) swimming. Dashed lines indicate the start and end of a BG cycle.

individuals to become separated and so increase their predation risk. RFF likely increases drag (James and Probyn, 1989; Sims, 1999), and so filter-feeding anchovies presumably alter some aspects of their swimming from normal swimming behavior to maintain speed and the integrity of the school, while maximizing net intake of food in the available time.

When not RFF or under predation threat, forage fish typically do not demonstrate steady swimming behavior, but engage in beat–glide (BG) swimming (Blake, 1983; Weihs and Webb, 1983). In this mode, fish accelerate using several tailbeats, straighten their body and enter a glide over which they decelerate to the initial speed, with the cycle then repeating (Fish et al., 1991; Weihs and Webb, 1983). This mode is common among migratory species, and is highly efficient over large distances (Fish et al., 1991; Weihs, 1974). This is because the hydrodynamical drag of a stretched out body is 1/3 to 1/5 that of a flexing body at equal speeds (Alexander, 1967). Thus, when schooling and feeding, anchovies apparently switch between highly efficient and highly inefficient swimming modes.

This is the first study to examine the kinematics of RFF in fish. Some swimming behaviors necessarily involve more use, or more frequent use, of the musculature, and so can be inferred to be more energetically costly. These include using a greater proportion of the body in swimming, a higher frequency of tailbeats and larger amplitude tailbeats. Here, using the northern anchovy, *Engraulis mordax*, we investigated the mechanisms and modifications to swimming kinematics that explain how filter-feeding fish switch between distinct swimming modes. Given the presumed decrease in streamlining during ram feeding, we hypothesized that in order to maintain their position within the school, anchovies would increase the frequency and amplitude of tailbeats to increase thrust and maintain speed under higher drag.

MATERIALS AND METHODS

Specimen maintenance

Engraulis mordax Girard 1854 were acquired from a commercial bait supplier in Oxnard, CA, USA, and held at Hopkins Marine Station, Pacific Grove, CA, USA, in a 3200 l circular tank (2.5 m diameter, 0.65 m deep) supplied with flowthrough seawater at 20 l min^{-1}, and fed 4 times daily on a mix of freeze-dried krill and commercial fish feed (2 mm sinking pellets, Skretting, UT, USA), at 0.4 g per individual per day. Fish constantly circled this tank as one large school. Approximately 200 were used for this study. This work was conducted under permit Stanford IACUC no. 28859 for working on fish.

Video capture

A 90×60 cm background was placed in the tank (Fig. 1B), illuminated by four 500 W halogen lights. A high-speed camera (Edgertronic, San Jose, CA, USA) was placed directly above, remotely triggered to avoid disturbance. Equipment was set up on the morning of each trial and left for several hours for fish to resume normal behavior. Before capturing video, the water supply was turned off to minimize surface disturbance and water currents.

Video recordings (120 frames s^{-1}) of BG and RFF were conducted on separate days. For BG, feeding was halted after the first feeding (06:00 h PST) and recordings were conducted in the afternoon. To induce RFF, specimens were not fed overnight, and in the morning the tank was seeded with finely ground krill mixed with seawater. After an initial increase in activity for approximately 15 min, larger particles were depleted and only smaller trace particles remained. Fish subsequently engaged in RFF for several hours thereafter. Videos were captured over several hours, with approximately 50 sequences of 5 s length captured for each behavior. These were later visually reviewed and individuals

Journal of Experimental Biology (2017) 220, 2717-2725 doi:10.1242/jeb.158337

Table 1. Swimming kinematics

Parameter	Abbreviation	Ram feeding	Beat–glide
Body length (cm)	L	10.66±0.52	10.50±0.43
Tailbeat amplitude (L)	A	0.21±0.01	0.23±0.04
Tailbeat amplitude – maximum (L)	A_{max}	0.25±0.03	0.27±0.03
Speed – mean (L s^{-1})	U	**2.29±0.20**	**2.80±0.28**
Speed – minimum (L s^{-1})	U_{min}	1.95±0.23	1.77±0.28
Speed – maximum (L s^{-1})	U_{max}	**2.58±0.29**	**3.92±0.48**
Distance per stroke (L stroke^{-1})	D_s	**0.66±0.06**	**2.01±1.05**
Tailbeat frequency (strokes s^{-1})	F	**3.51±0.24**	**3.89±0.42**
Yaw angle – mean (deg)	θ	5.75±0.82	5.87±1.04
Yaw angle – maximum (deg)	θ_{max}	**16.92±3.03**	**23.16±5.63**
Strouhal number	St	0.32±0.02	0.32±0.05

Data are means±s.d. A, U and D_s are all expressed as proportions of body length, L. Metrics that are significantly different (P<0.05) between groups based on ANOVA or Wilcoxon rank sum tests (see Materials and methods) are in bold.

Table 2. Midline kinematics

	Abbreviation	Ram feeding	Beat–glide
Pivot point location (distance from nose) (L)	pp	0.213±0.035	0.202±0.047
Amplitude at nose (L)	A_n	**0.055±0.014**	**0.076±0.019**
Amplitude at pivot point (L)	A_{pp}	0.040±0.009	0.045±0.013
Stride length (L stroke^{-1})	d	**0.608±0.055**	**0.729±0.085**
Propulsive wave velocity (L s^{-1})	w	**3.783±0.353**	**4.691±0.581**
Propulsive wave wavelength (L)	λ	**1.036±0.095**	**1.209±0.131**

Data are means±s.d. based on digitization of one full stroke for each of 12 specimens in each mode. A, w, pp and d are all expressed as proportions of body length, L. Metrics that are significantly different (P<0.05) between groups based on ANOVA are in bold.

displaying clear examples of RFF and BG (N=12 each) over gently curving paths unobscured by other specimens were identified for use in analysis (e.g. Fig. 1C).

Kinematics of swimming behavior

Videos were processed in Matlab (version 8.5 for Windows 10), using the package DLTdv5 (Hedrick, 2008). Three points were digitized in each frame; the nose (P_1), midpoint between the eyes (P_2) and base of the caudal fin (P_3) (Fig. 1A). All points were digitized manually.

Body length (L, cm; Table 1) and water depth (cm) were determined in ImageJ (v1.49, macOS) using image stacks extracted from videos. A scale bar was videoed at 5 cm depth intervals at each corner of the arena, and a formula to estimate the depth of the fish was derived based on the orthogonal offset of the shadows projected onto the tank bottom. Similarly, scale bar images and depths were used to determine L for each fish, defined as the distance from the nose to the base of the caudal fin (see Table S2). Depths varied from 3 to 16 cm above the tank bottom, and fish did not substantially alter depth while crossing the arena. No specimen used in analysis came closer than approximately 10 cm to the tank wall (with the majority no closer than 20 cm), which at these body lengths and tailbeat amplitudes is beyond where hydrodynamic 'wall effects' might occur (Webb, 1993) (see Table S2).

Tailbeat amplitude (A; Table 1) was calculated as the perpendicular distance of the base of the caudal fin (P_3) from a direction vector (**v**) in each frame (Fig. 1C, inset). Firstly, P_3 coordinates were used to derive a 4th order polynomial regression to model the path across the arena (e.g. Fig. 1D, arrowed lines). For each frame, **v** was calculated as a linear fit through the current coordinate and the five previous and five subsequent modeled coordinates. The perpendicular distance (a) of each P_3 coordinate from **v** was calculated for each frame (Fig. 1C, inset), and A was calculated as the sum of adjacent maximum a values. Overall mean A was calculated as the average amplitude of all tailbeats captured in the sequence, expressed as a proportion of L. Maximum amplitudes (A_{max}) were also calculated. For BG specimens, only full tailbeats were used, with half-tailbeats at the start or end of a bout excluded.

To determine speed (U, L s^{-1}; Table 1), the path of each fish across the arena was modeled as a 4th order polynomial regression similar to Fig. 1C but using P_2, the point displaying the least lateral movement. These coordinates removed the lateral movement (some was displayed along all parts of the body), allowing measurement of the distance covered between each frame. Speed was calculated as the sum of these frame-to-frame distances divided by the total number of frames (i.e. time), expressed as a proportion of body length (L s^{-1}). Frame-to-frame distances were converted into instantaneous speed, smoothed using a 20-point moving average, and used to determine minimum (U_{min}) and maximum (U_{max}) speed. Distance per stroke (D_s) was also calculated using these modeled data, for RFF over the entire sequence and for BG over a full stroking–glide cycle (e.g. Fig. 1D), and expressed as a proportion of body length (L stroke^{-1}).

Tailbeat frequency (F, strokes s^{-1}; Table 1) was determined using only full strokes, so in BG, F represents the frequency only during active stroking. A single tailbeat was defined as the maximum extent of the tail from the direction vector until the next maximum extent on the same side (e.g. Fig. 1C).

The yaw angle of the head (θ; Table 1) was assessed by analyzing the deviation of the body axis, defined as a straight line connecting the nose (P_1) and eye (P_2) points, from the vector of movement (**v**). For each frame, the angle of the P_1–P_2 axis to the direction vector **v** was determined (ϕ), and smoothed using a 10-point moving average. θ was calculated as the mean of these angles regardless of laterality, and θ_{max} as the maximum value. Strouhal numbers (St) were calculated as $F{\times}A{\times}U^{-1}$ (Lea et al., 2016).

Midline kinematics

To examine fine-scale body kinematics under each swimming mode, each specimen was subject to more detailed analysis. For each, 40 paired points on each side of the body were digitized on each frame for one full tailbeat (e.g. Fig. 1A); that is, from a left- or right-most tail extent until it has returned to the same position. All points were digitized manually. The geometric midpoints between each pair of lateral points were used to construct a midline of the fish for each frame (e.g. Fig. 2C). These midlines were aligned to the nose and rotated so the direction was parallel to the x-axis.

To determine where lateral motion was lowest, the pivot point (pp) was determined as the median of the five x-coordinates along the midline with lowest standard deviation in the y-dimension; that is, the five x-coordinates with the lowest overall lateral deviation. Amplitude at the nose (A_n) and pp (A_{pp}) was calculated as the difference between the minimum and maximum y-values at each, expressed as a proportion of L (Table 2).

Stride length (d, cm) was calculated as u/f, where u is swimming speed and f is tailbeat frequency for this particular stroke. u was

Journal of Experimental Biology (2017) 220, 2717-2725 doi:10.1242/jeb.158337

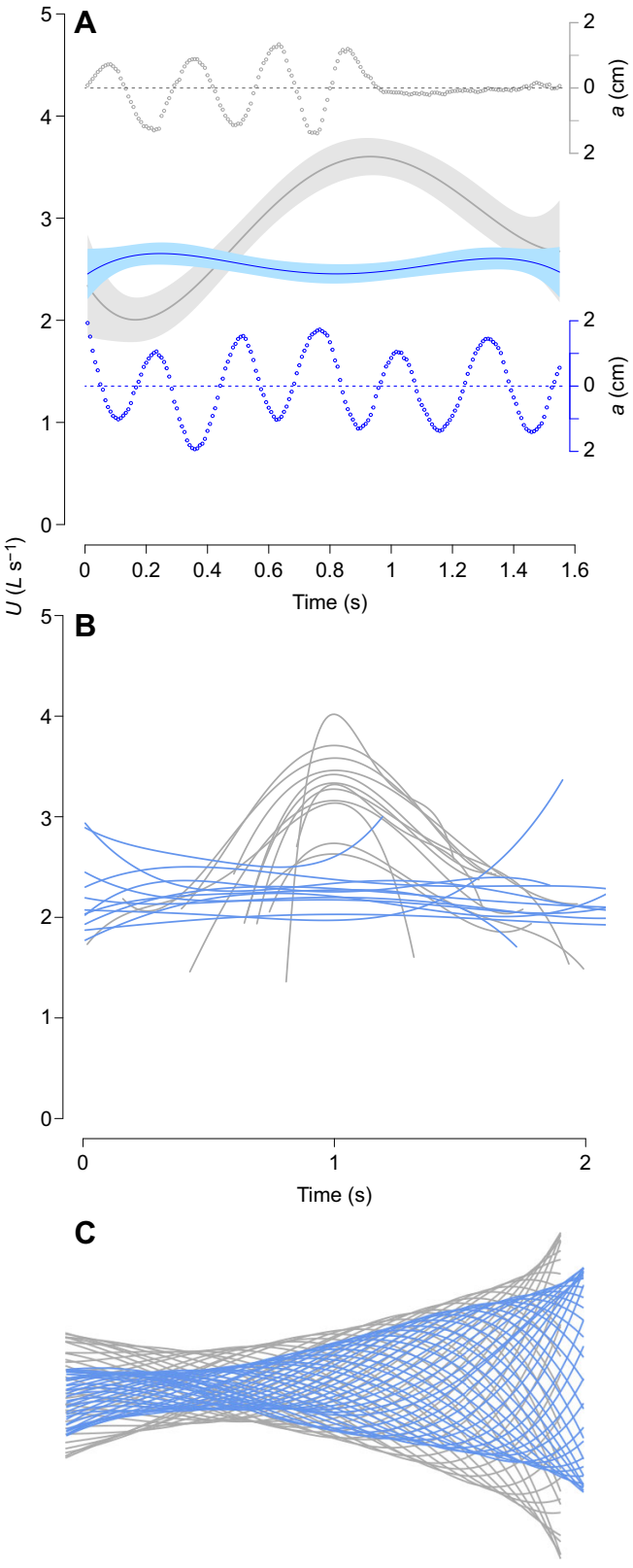

Fig. 2. Swimming kinematics. (A) Speed profiles for one example each of BG (gray open circles and line) and RFF (blue open circles and line). The BG plot shows one full BG cycle. The RFF example is an equivalent duration sequence. Top and bottom plots show the perpendicular distance (*a*) of the tail from the vector of movement in each frame, denoted by the dashed lines. The central plot shows speed (*U*; $L\ s^{-1}$) over the duration of the sequence. Lines are 4th order polynomial regressions through frame-to-frame calculated speeds (see Materials and methods), with shading indicating the 95% confidence intervals (CI) of the regressions. (B) Speed profiles for all specimens (*N*=12 each). Calculated as above, with CIs omitted for clarity. RFF is in blue, BG is in gray, with lines representing speed over a single BG cycle. For clarity, the BG profiles have been aligned with the maximum speed observed during the cycle at the 1 s time point. (C) Midlines from one full stroke for BG (gray) and RFF (blue) captured at 120 frames s^{-1}. For BG, there are 30 midlines and stroke duration is 0.25 s; for RFF, there are 36 midlines and stroke duration is 0.30 s. Midlines were aligned to the nose of the fish and rotated so the vector of movement was parallel to the *x*-axis. The same scale has been used for BG and RFF, but note the *y*-dimension has been slightly accentuated for clarity.

calculated as the mean of the frame-to-frame speed at the pivot point, and *f* as the time taken to complete the full stroke. Note, *d* is similar to D_s under RFF, but not under BG, as it does not include distance covered during gliding.

The velocity of the propulsive wave along the body (*w*) was determined by identifying in each frame the most lateral *y*-value of the body and using the associated *x*-value to calculate the distance this moved per frame, and therefore its velocity, expressed as a proportion of body length ($L\ s^{-1}$; Table 2; Fig. S1; Shadwick and Gemballa, 2006). The wavelength (λ) of the propulsive wave was calculated as *w*/*f* (Table 2).

Statistical analysis

Data analysis and statistical tests were conducted in R (http://www.R-project.org/). Differences between RFF and BG groups were examined using unpaired, two-tailed analysis of variance (ANOVA). All data met the normality assumptions of ANOVA (Shapiro–Wilk test); however, two metrics (*A* and D_s) failed the homogeneity of variance assumptions of ANOVA (Bartlett test), so were examined using the non-parametric Wilcoxon rank sum test. Pairwise linear dependence between measured parameters (*A*, θ, *U*, *F*, D_s) was assessed using Pearson correlations. All measurements of variability are standard deviation (s.d.).

RESULTS

Swimming kinematics

Body length (*L*) was not significantly different between RFF and BG groups (ANOVA, $F_{1,22}$=0.66, *P*=0.42), with a mean value across all 24 specimens of 10.58±0.47 cm.

In general, although we chose individuals displaying the most typical BG behavior, these showed much greater variance than RFF swimmers in most kinematic metrics (Fig. 3, Table 1). However, tailbeat amplitudes (*A*) were not significantly different between the two behaviors (Wilcoxon rank sum test, *W*=96, *P*=0.18). In BG, *A* tended to be slightly larger, but also more variable (Table 1). This is somewhat expected, as stroking bouts in BG tended to begin with smaller amplitude tailbeats (e.g. Fig. 1D), as opposed to the highly regular amplitudes characterized by RFF (e.g. Fig. 1C). Maximum tailbeat amplitudes (A_{max}) were also not significantly different between the two modes ($F_{1,22}$=3.22, *P*=0.09).

Speed (*U*) was highly significantly different between modes ($F_{1,22}$=26.7, *P*<0.0001); BG were around 20% faster at 2.80 $L\ s^{-1}$ versus 2.29 $L\ s^{-1}$ for RFF. Again, however, there was much more variance under BG (Fig. 2); as well as being faster on average, U_{min} and U_{max} were lower and higher than in RFF, although this was significant only for U_{max} (U_{min}, $F_{1,22}$=2.82, *P*=0.11; U_{max}, $F_{1,22}$=67.0, *P*<0.0001). Peak speeds in BG were up to twice those under RFF (Fig. 2), being highest at the end of stroking bouts, ranging from 4.53 to 1.36 $L\ s^{-1}$ at the end of a glide in one specimen. RFF speeds were highly consistent, varying among individuals by an average of only 13% around the mean.

Journal of Experimental Biology (2017) 220, 2717-2725 doi:10.1242/jeb.158337

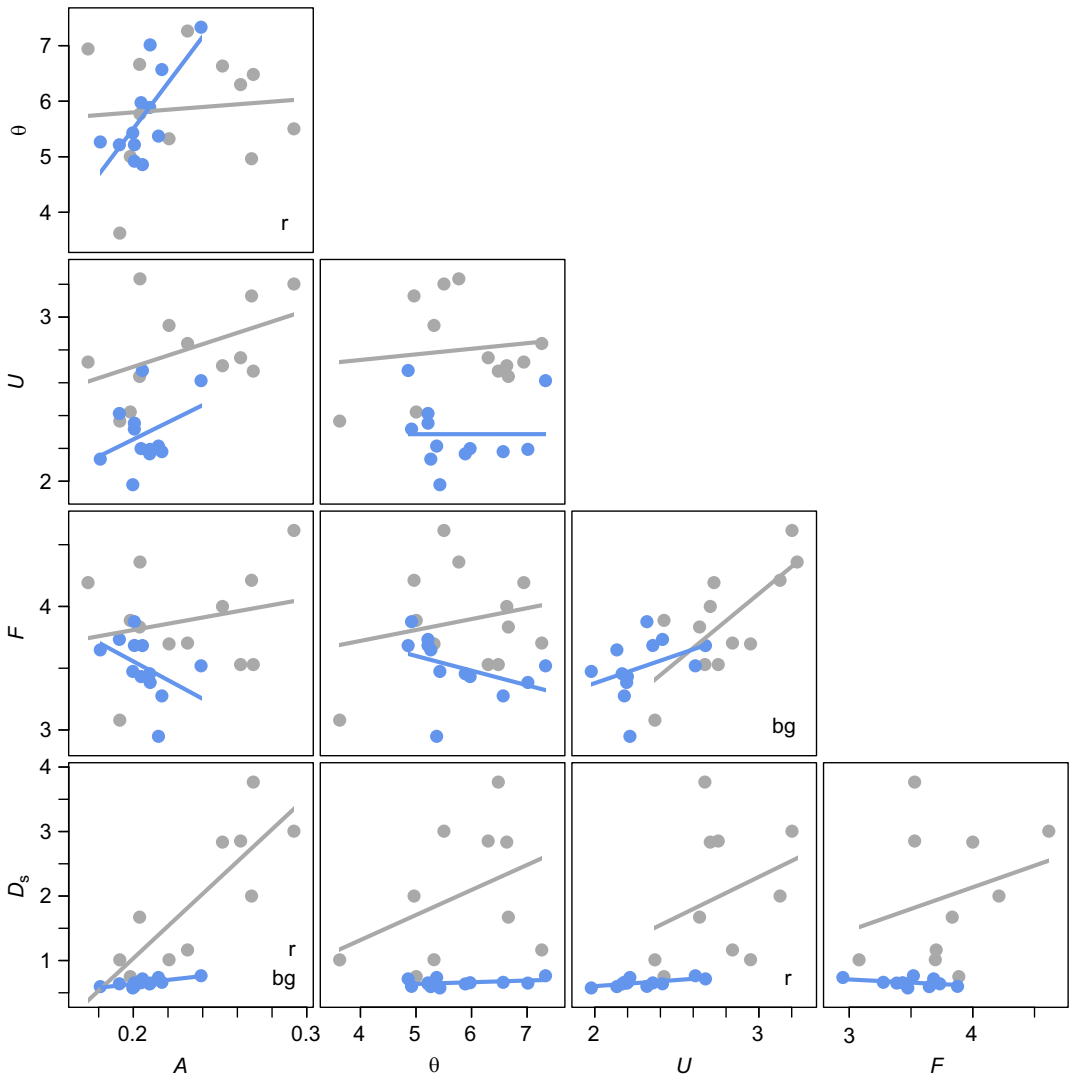

Fig. 3. Correlation matrix for swimming kinematic parameters. Gray dots and lines are BG, blue dots and lines are RFF; *N*=12 for each mode. Lines are linear regressions and are included only to visualize trends between parameters. Significantly correlated parameters (based on Pearson correlations, see Materials and methods) are indicated in the bottom right corners: *r*, significant correlation under RFF; bg, significant correlation under BG. *A*, tailbeat amplitude (*L*); θ, yaw angle (deg); *U*, speed (*L* s^{-1}); *F*, tailbeat frequency (strokes s^{-1}); D_s, distance covered per stroke (*L* $stroke^{-1}$).

Tailbeat frequency (*F*) was significantly different between the two behaviors ($F_{1,22}$=7.2, *P*=0.01). BG swimmers stroked at a higher *F* (3.89 strokes s^{-1}, Table 1) than in RFF (3.51 strokes s^{-1}). Again, there was more variability under BG, with some stroking rapidly between glides (up to 4.62 strokes s^{-1}), and others less rapidly (3.08 strokes s^{-1}). Under RFF, *F* was highly consistent; in one specimen, *F* was 2.95 strokes s^{-1}, but in the remaining 11 it varied only between 3.27 to 3.88 strokes s^{-1}. Distance covered per stroke (D_s) differed radically between the two behaviors (*W*=119, *P*<0.0001), with BG swimmers covering over 3 times the distance for each tailbeat compared with RFF swimmers (BG, 2.01 *L* $stroke^{-1}$; RFF, 0.66 *L* $stroke^{-1}$). Strouhal numbers did not differ between BG and RFF ($F_{1,22}$=0.03, *P*=0.87), with equal mean values in each (BG: *St*=0.32±0.05; RFF: *St*=0.32±0.02; Table 1).

Correlations between swimming kinematic parameters

Two parameters, *A* and D_s, were significantly correlated under both swimming modes; larger amplitude tailbeats resulted in larger distance covered in both modes, though the relationship under BG was much stronger (Fig. 3; see Table S1 for correlation values).

Under RFF, there were two significant positive correlations which were not significant under BG; between *A* and θ (Pearson, *r*=0.72, *P*=0.01) and between *U* and D_s (*r*=0.67, *P*=0.02). There were several additional strong, though non-significant, relationships: positive correlations between *A* and *U*, and between *F* and *U*; and a negative correlation between *A* and *F* (Table S1). Under BG, there was a significant positive correlation between *U* and *F* (*r*=0.73, *P*=0.01); additional non-significant but strong positive relationships included that between *A* and *U*, as in RFF.

There were some contrasting relationships across swimming modes. For instance, the relationship between *A* and *F* was strongly negative in RFF (*r*=−0.44, *P*=0.15), but positive in BG (*r*=0.22, *P*=0.48). Similarly, the relationship between θ and *F* was strongly negative in RFF (*r*=−0.40, *P*=0.20) but positive in BG (*r*=0.22, *P*=0.49).

Midline kinematics

We note that for BG, although we generally selected relatively uniform tailbeats from the middle of stroking bouts, BG tailbeat kinematics differed substantially even within a stroking bout, which

Journal of Experimental Biology (2017) 220, 2717-2725 doi:10.1242/jeb.158337

may be due to the unsteady nature of this behavior as the body accelerates (e.g. Fig. 2A). Therefore, the following metrics in BG should be considered as instantaneous values at a particular moment in the highly variable BG cycle. As RFF swimming is much more consistent in all kinematic metrics, these values can be considered more generally.

Midline kinematics differed substantially between behaviors and suggest that under RFF anchovies tend to maintain a straightened body form, with lower overall lateral movement at any part of the body when compared with that under BG (Fig. 2C, Table 2).

The location of the pivot point (pp), the region of the body that displays the least lateral movement, was marginally (not significantly; $F_{1,22}$=0.46, P=0.051) further forward under RFF. Amplitude at the pp (A_{pp}) did not significantly differ between RFF and BG ($F_{1,22}$=1.44, P=0.24). However, under RFF, lateral movement around the head is significantly reduced compared with that under BG, the A_n under RFF being close in value to A_{pp} (0.055 L versus 0.040 L), and 22% of the tail amplitude (A). This contrasts with values under BG, with A_n being substantially larger than A_{pp} (0.076 L versus 0.045 L), and 33% of A. A_n is also significantly greater overall in BG compared with that in RFF ($F_{1,22}$=9.89, P=0.005). This, allied with lower amplitudes at all parts of the body (Fig. 2C, Tables 1 and 2), and lower maximum yaw angle (Table 1), suggests that under RFF the body, and particularly the anterior portion, is kept much straighter to the direction of travel.

Both the velocity (w) and wavelength (λ) of the propulsive wave along the body were significantly different between behaviors (w, $F_{1,22}$=21.4, P=0.0001; λ, $F_{1,22}$=13.73, P=0.001; Table 2). The observation that RFF under-utilizes the anterior portion of the body compared with BG, as suggested by lower lateral movement, is also supported by λ being shorter in RFF (1.036 L) than in BG (1.209 L; Table 2), suggesting that under BG more of the body is used in propulsion.

Stride length (d) was significantly lower under RFF swimming ($F_{1,22}$=17.42, P=0.0004), indicating a lesser distance covered during active stroking.

DISCUSSION

This is the first study to examine the alterations to fish swimming kinematics associated with RFF. *Engraulis mordax* displays a high degree of plasticity in swimming kinematics, as shown by the large variability in most kinematic parameters under BG swimming. However, under RFF, there appears to be a very narrow range of kinematic behaviors, with low scope for variation within these. Swimming under RFF in *E. mordax* is characterized by a decrease in the use of the anterior part of the body (Fig. 2C). Contrary to expectations, tailbeat amplitudes (A) did not differ between the behaviors, and in fact were slightly lower under RFF, though not significantly so (Table 1). Tailbeat frequencies (F) and swimming speed (U) did differ significantly, but not in the manner we hypothesized; instead, under RFF, F was significantly lower, and U was significantly decreased by around 18% (Table 1).

Ram feeding results in distinct changes to swimming kinematics; the body is kept anteriorly straighter, with the major swimming effort moved posteriorly, as shown by the lower wavelength (λ) of the body propulsive wave (Table 2). Lateral deviation at all parts of the body is generally lower, but particularly around the head (Fig. 2C). The relatively low variation in body kinematics under ram swimming implies a narrow range of circumstances where it might be energetically beneficial to feed with swimming-induced flows. Some studies hint at this; *E. mordax* will only start ram feeding when food particles in the water reach a certain minimum size or sufficient concentration (Hunter and Dorr, 1982), as ram feeding is more energetically costly (Durbin et al., 1981; James and Probyn, 1989; Macy et al., 1999).

Frequency and amplitude

Fish can increase thrust by increasing tailbeat frequency (F) or amplitude (A). Generally, swimming speed (U) may be modulated at low speeds by altering F or A, while at moderate to higher speeds, it is modulated only by changes to F (Bainbridge, 1958; Webb, 1971). However, A often remains relatively constant at all speeds (Webb et al., 1984). Thus, changes to F are typically thought to be the main mechanism by which fish modulate their speed. The relationship between F and U is typically strongly positive, and often linear (Bainbridge, 1958; Stevens, 1979; Webb et al., 1984), but may also be a power function (Steinhausen et al., 2005). Here, we saw a significant, linear positive relationship between F and U under BG, but a weaker, non-significant relationship between these parameters under RFF (Fig. 3). This suggests that the presumed high drag of an open mouth during RFF may somewhat limit the increases in speed that would otherwise be seen given the increase in F.

A was also positively related to U under both modes, as might be expected at these relatively low speeds (Bainbridge, 1958; Webb, 1971). It appears that at these schooling speeds, *E. mordax* uses a combination of alterations to both F and A to modulate U (Fig. 3). There were, however, contrasting relationships between A and F under the different modes. During RFF, the relationship was negative, so there appears to be a trade-off between F and A (Fig. 3) and *E. mordax* increase either F or A to maintain thrust, but increasing both may not be possible, or may be too energetically costly. In BG, there appears to be little to no relationship between F and A (Fig. 3), similar to results found in other studies (Bainbridge, 1958; McHenry et al., 1995).

Distance

The different costs of swimming between the two modes is most starkly illustrated by the distance covered per stroke (D_s), which was significantly higher in BG swimming compared with RFF, with over 3 times the distance covered for the same number of tailbeats (Table 1). Stride length (d), a similar metric but examining only the distance covered during active stroking, was also significantly higher under BG (Table 2). The relationship between D_s and the other metrics is shown in Fig. 3 (bottom row). D_s was significantly positively related to A under both modes, but much more strongly under BG; in this mode, increases in A greatly increase the distance covered. By contrast, the relationship between F and D_s, while positive, is much less strong. This is opposite to how F and A affect speed (U) as discussed above, where F is the dominant influence. It appears that under BG swimming, A is the dominant influence on D_s, while F is the dominant influence on U. Under RFF, changes to either only very marginally affect D_s (Fig. 3).

Speed

Speed (U) appears to be limited under ram filter feeding (Fig. 3). This somewhat contradicts several other studies which suggest increased speed under RFF, including in *E. mordax* (James and Probyn, 1989; Pepin et al., 1988; Rice and Hale, 2010). These observations may be 'feeding frenzy' responses to the immediate detection of food and may represent particulate feeding rather than filter feeding. In *E. mordax*, these last approximately 5–10 min, after which typical schooling behavior is resumed (N.C. and J.A.G., personal observation; James and Probyn, 1989), although these

Journal of Experimental Biology

higher speeds may persist for a considerable time afterwards (James and Probyn, 1989). Such responses are likely competitive, resulting from the need for individuals to quickly take advantage of infrequently encountered aggregations of prey (Hunter and Dorr, 1982; James and Probyn, 1989). If these behaviors reflect true RFF, as opposed to particulate feeding, it does suggest there are no biomechanical or hydrodynamic constraints on faster speeds with the filtering apparatus deployed. However, maintaining such speeds may be energetically costly; RFF in general is associated with increased metabolic costs of movement, hypothesized as resulting from the need to overcome increased drag (Durbin et al., 1981; James and Probyn, 1989; Macy et al., 1999; Simon et al., 2009; Sims, 2000). However, in circumstances of high food availability, the expenditure under such higher speeds may be energetically beneficial (James and Probyn, 1989; Sims, 1999).

The lower speeds we observed may be explained through several mechanisms. It is possible that the efficacy of the filtering apparatus is bounded by an upper speed limit; above a certain threshold of speed, any filter or mesh will act as a solid rather than porous surface (Fujita, 1956) and, rather than filter, push a bolus of water ahead of it (Sanderson and Wassersug, 1993). Swimming fish typically use the reduced pressure behind the operculum or gill slits to draw water out, induced by the Bernouli effect (Sanderson and Wassersug, 1993; Vogel, 1994), but if there is an upper, biologically relevant speed at which this fails in anchovies, it is unknown at this time. RFF has, however, been reported in the anchovy *Engraulis capensis* at speeds over 3 times higher than we observed in this study (see fig.1 of James and Probyn, 1989), for prolonged periods of up to 2 h following the introduction of food. It seems unlikely this would occur if higher speeds resulted in food being pushed away from the mouth by such a bolus effect. Alternatively, the filtering apparatus of most ram filter feeders is flexible (Sanderson and Wassersug, 1993), so under the hydrodynamic forces that come with higher speeds it is also possible that the delicate filtering apparatus of anchovies is instead deformed, with partial or total lack of function. Under this scenario, lower speeds are selected to avoid this occurring. Another explanation, however, is that in ram filter feeders, swimming speeds are selected to balance energetic costs and benefits, related to the amount of food available (Durbin et al., 1981; Macy et al., 1999; Sanderson and Wassersug, 1993; Simon et al., 2009; Sims, 1999, 2000). The mean speed we observed under RFF (0.24 m s^{-1}, shown as a proportion of L in Table 1) is very close to the hypothesized optimum feeding speed at 15°C (coincidentally the temperature used here) for filter feeding of 0.26 m s^{-1} ($0.69L^{0.43}$) (Weihs and Webb, 1983). There is further support through the Strouhal numbers we observed, 0.32 in both modes, being within the range of 0.25 to 0.35 hypothesized to maximize propulsive efficiency (Eloy, 2012). The decrease in speed during routine RFF may therefore be due to one or a combination of these aspects: a feeding strategy that balances energy expenditure and intake in conditions of low food concentrations, or because the hydrodynamics of filtering at higher speeds would cause the filtering process to fail or become sub-optimal.

Reduced RFF speeds are also observed in other species, including those greatly different in size such as basking sharks (18–50% decrease; Sims, 1999), whale sharks (Heyman et al., 2001) and bowhead whales (Simon et al., 2009). Basking sharks are thought to modulate their speeds predictably in response to prey density (Sims, 1999), but whether anchovies do so, beyond initial frenzy type responses, is unknown and warrants further study. Schooling fish are in a unique position where collective behaviors are ecologically important; maintaining school integrity is crucial in terms of both energetics and reducing predation risk (Herskin and Steffensen, 1998; Marras et al., 2015; Nadler et al., 2016; Weihs and Webb, 1983). While individuals may risk falling out of the school under RFF as a result of lower speeds, if the rest of the school is also engaging in sporadic filter feeding, school integrity may not be compromised but instead the whole school may travel at a lower average speed. Anchovy schools are known to migrate over large distances (Giannoulaki et al., 2014). Our data suggest that schools engaging in sporadic or continuous RFF will travel more slowly than those targeting larger prey, with implications for models of species distributions under different environmental conditions.

It should be noted that, as a result of turning, fish swimming on an arc expend more energy than those swimming in a straight line (Weihs, 1981). Effectively, this manifests as a reduction in speed for the same amount of effort (Domenici et al., 2000). Therefore, our experimental setup, which involved fish swimming on a curving path, would be expected to affect the speeds observed. This effect can, however, be easily calculated using the fish length and the radius of the arc (Domenici et al., 2000; He and Wardle, 1988). Here, we estimated that along a straight path these fish may have swum faster by between 6% and 12% (calculations not shown), a factor lower in magnitude than that observed in similar studies (e.g. 16%; Domenici et al., 2000). However, we also note that individuals within fish schools may also swim along curved paths in order to exploit patchy food resources, or take up different positions within the school (Marras et al., 2015; Nadler et al., 2016), so our experimental design may have some direct relevance to the natural system.

Body kinematics

While mean speeds under BG swimming were consistently higher than under RFF, instantaneous speeds, acceleration–deceleration profiles and cycle lengths were highly variable (Fig. 2B), again demonstrating the plasticity in routine swimming kinematics. Primarily, this variability was driven by differences between individuals in the number of strokes taken before glides. Some individuals utilized short cycles, with only a single strong tailbeat, and high acceleration and deceleration before the next cycle, while others took up to four or five weaker tailbeats with lower amplitude acceleration and deceleration profiles, and longer duration cycles. Our experimental setup did not allow us to follow individual fish over several cycles, so it is not known whether these behaviors are specific to individuals, or whether they vary their cycle lengths over time, and this is an aspect that requires further study. It bears repeating that the midline analysis in BG (though not of the broader swimming kinematics which used all full strokes in a cycle) was generally based upon strokes from the middle of a stroking bout. Just as stroking bouts varied substantially in kinematic characteristics between individuals (Table 1, Fig. 2B), individual strokes under BG swimming also varied substantially within individuals; stroking bouts tended to begin with low-amplitude strokes, with amplitude getting progressively larger until the commencement of the glide (e.g. Fig. 1D). Therefore, any consideration of the midline kinematics of these strokes should be regarded with that in mind; any particular stroke in BG swimming could be regarded as atypical while the body is not in a steady state.

It is, however, clear from the midline kinematics (Table 2, Fig. 2C) that under RFF less of the body is used in forward propulsion; the anterior is kept straighter with very limited lateral movement at the head, and overall lower lateral movement in all parts of the body. The maximum yaw angle (θ_{max}) is also significantly lower (Table 1), again indicating lower lateral head movement. Why the body kinematics change in this manner or

whether it is a passive or active process is not clear. It may be because keeping the filtering apparatus straighter to the direction of movement is optimal in processing the water column and thus capturing food particles, or that the particular morphology of the filtering apparatus under forward thrust constrains lateral movement. Alternatively, it may be an active response to minimize the presumed increased drag forces imposed by the filtering apparatus under this swimming mode (Sanderson and Wassersug, 1993). Supportive of this hypothesis is that yaw angle is highly significantly positively related to tailbeat amplitude under RFF, but not under BG (Fig. 3, θ versus *A*; Table S1). Under RFF, even a minor increase in amplitude results in a large increase in yaw angle. The drag of a flexing body is 3–5 times greater than that of a straight body at equal speed (Alexander, 1967), so this suggests tailbeat amplitude under RFF may be kept low to avoid flexing of the anterior of the body and further increasing drag.

Engraulis mordax switches between swimming modes that are apparently diametrically opposite; highly energy efficient, low-drag BG and RFF, a mode proposed as more costly because of the need to overcome increased drag (James and Probyn, 1989; Sanderson and Wassersug, 1993; Sims, 1999, 2000). While other fish vary swimming kinematics to alter speed or efficiency, filter feeders uniquely trade off these with the acquisition of energy in processing a larger volume of water over the filtering apparatus. *Engraulis mordax* displays a high degree of plasticity in body kinematics under routine swimming behavior, but when RFF, these are constrained within an extremely narrow range, and less of the body is used in propulsion. Our results suggest that hydrodynamic physical constraints may limit behavioral options during foraging, resulting in lower swimming speeds.

Acknowledgements
Many thanks to Joe Welsh and John O'Sullivan (Monterey Bay Aquarium) for help sourcing specimens, Kelly Barr (UCLA) for help with the experimental set-up, Natasha Maier Batista (Stanford University) for assistance with digitizing the video, and Jody Beers (Hopkins Marine Station) for help with specimen maintenance. Paolo Domenici and Jean Potvin provided helpful comments on an earlier version of the manuscript. Two anonymous reviewers provided input which greatly improved the final version of the manuscript. This work was conducted under permit Stanford IACUC #28859 for working on fish.

Competing interests
The authors declare no competing or financial interests.

Author contributions
Conceptualization: N.C., J.A.G.; Writing - original draft: N.C.; Writing - review & editing: J.A.G.

Funding
This research received no specific grant from any funding agency in the public, commercial or not-for-profit sectors.

Supplementary information
Supplementary information available online at
http://jeb.biologists.org/lookup/doi/10.1242/jeb.158337.supplemental

References
Alexander, R. M. (1967). *Functional Design in Fishes*. London: Hutchinson Univ. Library.
Bainbridge, R. (1958). The speed of swimming of fish as related to size and the frequency and amplitude of the tail beat. *J. Exp. Biol.* **35**, 109-133.
Blake, R. W. (1983). Functional design and burst-and-coast swimming in fishes. *Can. J. Zool.* **61**, 2491-2494.
Blake, R. W. (2004). Fish functional design and swimming performance. *J. Fish Biol.* **65**, 1193-1222.
Crowder, L. B. (1985). Optimal foraging and feeding mode shifts in fishes. *Environ. Biol. Fishes* **12**, 57-62.
Cury, P., Bakun, A., Crawford, R. J. M., Jarre, A., Quiñones, R. A., Shannon, L. J. and Verheye, H. M. (2000). Small pelagics in upwelling systems: patterns of interaction and structural changes in "wasp-waist" ecosystems. *ICES J. Mar. Sci.* **57**, 603-618.
Domenici, P. (2003). Habitat, body design and the swimming performance of fish. In *Vertebrate Biomechanics and Evolution* (ed. V. L. Bels, J. P. Gasc and A. Casinos), pp. 137-160. Oxford, UK: BIOS Scientific.
Domenici, P., Steffensen, J. F. and Batty, R. S. (2000). The effect of progressive hypoxia on swimming activity and schooling in Atlantic herring. *J. Fish Biol.* **57**, 1526-1538.
Domenici, P., Wilson, A. D. M., Kurvers, R. H. J. M., Marras, S., Herbert-Read, J. E., Steffensen, J. F., Krause, S., Viblanc, P. E., Couillaud, P. and Krause, J. (2014). How sailfish use their bills to capture schooling prey. *Proc. R. Soc. Lond. B Biol. Sci.* **281**.
Durbin, A. G., Durbin, E. G., Verity, P. G. and Smayda, T. J. (1981). Voluntary swimming speeds and respiration rates of a filter-feeding planktivore, the Atlantic Menhadden, *Brevortia tyrannus*. *Fish. Bull.* **78**, 877-886.
Eloy, C. (2012). Optimal Strouhal number for swimming animals. *J. Fluids Struct.* **30**, 205-218.
Fish, F. E., Fegely, J. F. and Xanthopoulos, C. J. (1991). Burst-and-coast swimming in schooling fish (Notemigonus crysoleucas) with implications for energy economy. *Comp. Biochem. Physiol.* **100**, 633-637.
Fleming, A. H., Clark, C. T., Calambokidis, J. and Barlow, J. (2016). Humpback whale diets respond to variance in ocean climate and ecosystem conditions in the California Current. *Glob. Chang. Biol.* **22**, 1214-1224.
Fujita, H. (1956). The collection efficiency of a plankton net. *Res. Popul. Ecol.* **3**, 8-15.
Gende, S. M. and Sigler, M. F. (2006). Persistence of forage fish "hot spots" and its association with foraging Steller sea lions (Eumetopias jubatus) in southeast Alaska. *Deep Sea Res. Part II Top. Stud. Oceanogr.* **53**, 432-441.
Giannoulaki, M., Schismenou, E., Pyrounaki, M.-M. and Tsagarakis, K. (2014). Habitat characterization and migrations. In *Biology and Ecology of Sardines and Anchovies* (ed. K. Ganias), pp. 191-241. Boca Raton, FL: CRC Press.
Gibson, R. N. and Ezzi, I. A. (1985). Effect of particle concentration on filter- and particulate-feeding in the herring Clupea harengus. *Mar. Biol.* **88**, 109-116.
Gibson, R. N. and Ezzi, I. A. (1992). The relative profitability of particulate- and filter-feeding in the herring, *Clupea harengus* L. *J. Fish Biol.* **40**, 577-590.
Handegard, N. O., Boswell, K. M., Ioannou, C. C., Leblanc, S. P., Tjøstheim, D. B. and Couzin, I. D. (2012). The dynamics of coordinated group hunting and collective information transfer among schooling prey. *Curr. Biol.* **22**, 1213-1217.
He, P. and Wardle, C. S. (1988). Endurance at intermediate swimming speeds of Atlantic mackerel, Scomber scombrus L., herring, Clupea harengus L., and saithe, Pollachius virens L. *J. Fish Biol.* **33**, 255-266.
Hedrick, T. L. (2008). Software techniques for two- and three-dimensional kinematic measurements of biological and biomimetic systems. *Bioinspir. Biomim.* **3**, 34001.
Herbert-Read, J. E., Romanczuk, P., Krause, S., Strömbom, D., Couillaud, P., Domenici, P., Kurvers, R. H., Marras, S., Steffensen, J. F., Wilson, A. D. et al. (2016). Proto-cooperation: Group hunting sailfish improve hunting success by alternating attacks on grouping prey. *Proc. R. Soc. B Biol. Sci.* **283**, 1-24
Herskin, J. and Steffensen, J. F. (1998). Energy savings in sea bass swimming in a school: measurements of tail beat frequency and oxygen consumption at different swimming speeds. *J. Fish Biol.* **53**, 366-376.
Heyman, W. D., Graham, R. T., Kjerfve, B. and Johannes, R. E. (2001). Whale sharks Rhincodon typus aggregate to feed on fish spawn in Belize. *Mar. Ecol. Prog. Ser.* **215**, 275-282.
Hunter, J. R. and Dorr, H. (1982). Thresholds for filter feeding in Northern anchovy, Engraulis mordax. *Calif. Coop. Ocean. Fish. Investig. Rep.* **23**, 198-204.
Ioannou, C. C., Guttal, V. and Couzin, I. D. (2012). Predatory fish select for coordinated collective motion in virtual prey. *Science*, **337**, 1218919.
James, A. G. and Probyn, T. (1989). The relationship between respiration rate, swimming speed and feeding behaviour in the Cape anchovy Engraulis capensis Gilchrist. *J. Exp. Mar. Biol. Ecol.* **131**, 81-100.
Lea, J. M. D., Keen, A. N., Nudds, R. L. and Shiels, H. A. (2016). Kinematics and energetics of swimming performance during acute warming in brown trout *Salmo trutta*. *J. Fish Biol.* **88**, 403-417.
Macy, W. K., Durbin, A. G. and Durbin, E. G. (1999). Metabolic rate in relation to temperature and swimming speed, and the cost of filter feeding in Atlantic menhaden, Brevoortia tyrannus. *Fish. Bull.* **97**, 282-293.
Marras, S., Killen, S. S., Lindström, J., McKenzie, D. J., Steffensen, J. F. and Domenici, P. (2015). Fish swimming in schools save energy regardless of their spatial position. *Behav. Ecol. Sociobiol.* **69**, 219-226.
McHenry, M. J., Pell, C. A. and Long, J. H. (1995). Mechanical control of swimming speed: stiffness and axial wave form in undulating fish models. *J. Exp. Biol.* **198**, 2293-2305.
Nadler, L. E., Killen, S. S., McClure, E. C., Munday, P. L. and McCormick, M. I. (2016). Shoaling reduces metabolic rate in a gregarious coral reef fish species. *J. Exp. Biol.* **219**, 2802-2805.
Neill, S. R. S. J. and Cullen, J. M. (1974). Experiments on whether schooling by their prey affects the hunting behaviour of cephalopods and fish predators. *J. Zool. Lond.* **172**, 549-569.

Pepin, P., Koslow, J. A. and Pearre, S. Jr. (1988). Laboratory study of foraging by Atlantic mackerel, *Scomber scombrus*, on natural zooplankton assemblages. *Can. J. Fish. Aquat. Sci.* **45**, 879-887.
Rice, A. N. and Hale, M. E. (2010). Roles of locomotion in feeding. In *Fish Locomotion: An Eco-ethological Perspective* (ed. P. Domenici and B. G. Kapoor), pp. 171-199. Enfield, NH, USA: Science Publishers.
Rieucau, G., De Robertis, A., Boswell, K. M. and Handegard, N. O. (2014). School density affects the strength of collective avoidance responses in wild-caught Atlantic herring Clupea harengus : a simulated predator encounter experiment. *J. Fish Biol.* **85**, 1650-1664.
Sanderson, S. L. and Wassersug, R. (1993). Convergent and alternative designs for vertebrate suspension feeding. In *The Skull*, Vol. 3 (ed. J. Hanken and B. K. Hall), pp. 37-112. Chicago: University of Chicago Press.
Schweigert, J. F., Boldt, J. L., Flostrand, L. and Cleary, J. S. (2010). A review of factors limiting recovery of Pacific herring stocks in Canada. *ICES J. Mar. Sci.* **67**, 1903-1913.
Shadwick, R. E. and Gemballa, S. (2006). Structure, kinematics and muscle dynamics in undulatory swimming. In *Fish Biomechanics* (ed. R. E. Shadwick and G. V. Lauder), pp. 241-280. San Diego: Academic Press/Elsevier.
Simon, M., Johnson, M., Tyack, P. and Madsen, P. T. (2009). Behaviour and kinematics of continuous ram filtration in bowhead whales (Balaena mysticetus). *Proc. R. Soc. Lond. B Biol. Sci.* **276**, 3819-3828.
Sims, D. W. (1999). Threshold foraging behaviour of basking sharks on zooplankton: life on an energetic knife-edge? *Proc. R. Soc. B Biol. Sci.* **266**, 1437-1443.
Sims, D. W. (2000). Filter-feeding and cruising swimming speeds of basking sharks compared with optimal models: they filter-feed slower than predicted for their size. *J. Exp. Mar. Biol. Ecol.* **249**, 65-76.
Steinhausen, M. F., Steffensen, J. F. and Andersen, N. G. (2005). Tail beat frequency as a predictor of swimming speed and oxygen consumption of saithe (Pollachius virens) and whiting (Merlangius merlangus) during forced swimming. *Mar. Biol.* **148**, 197-204.
Stevens, E. D. (1979). The effect of temperature on tail beat frequency of fish swimming at constant velocity. *Can. J. Zool.* **57**, 1628-1635.
Vogel, S. (1994). *Life in Moving Fluids: The Physical Biology of Flow*. 2nd edn. Princeton, NJ: Princeton University Press.
Webb, P. W. (1971). The swimming energetics of trout. *J. Exp. Biol.* **55**, 489-520.
Webb, P. W. (1984). Body form, locomotion and foraging in aquatic vertebrates. *Am. Zool.* **24**, 107-120.
Webb, P. W. (1993). The effect of solid and porous channel walls on steady swimming of steelhead trout *Oncorhynchus mykiss*. *J. Exp. Biol.* **178**, 97-108.
Webb, P. W., Kostecki, P. T. and Stevens, E. D. (1984). The effect of size and swimming speed on locomotor kinematics of rainbow trout. *J. Exp. Biol.* **109**, 77-95.
Weihs, D. (1974). Energetic advantages of burst swimming of fish. *J. Theor. Biol.* **48**, 215-229.
Weihs, D. (1981). Effects of swimming path curvature on the energetics of fish motion. *Fish. Bull.* **79**, 171-176.
Weihs, D. and Webb, P. W. (1983). Optimization of locomotion. In *Fish Biomechanics* (ed. P. W. Webb and D. Weihs), pp. 339-371. New York: Praeger.

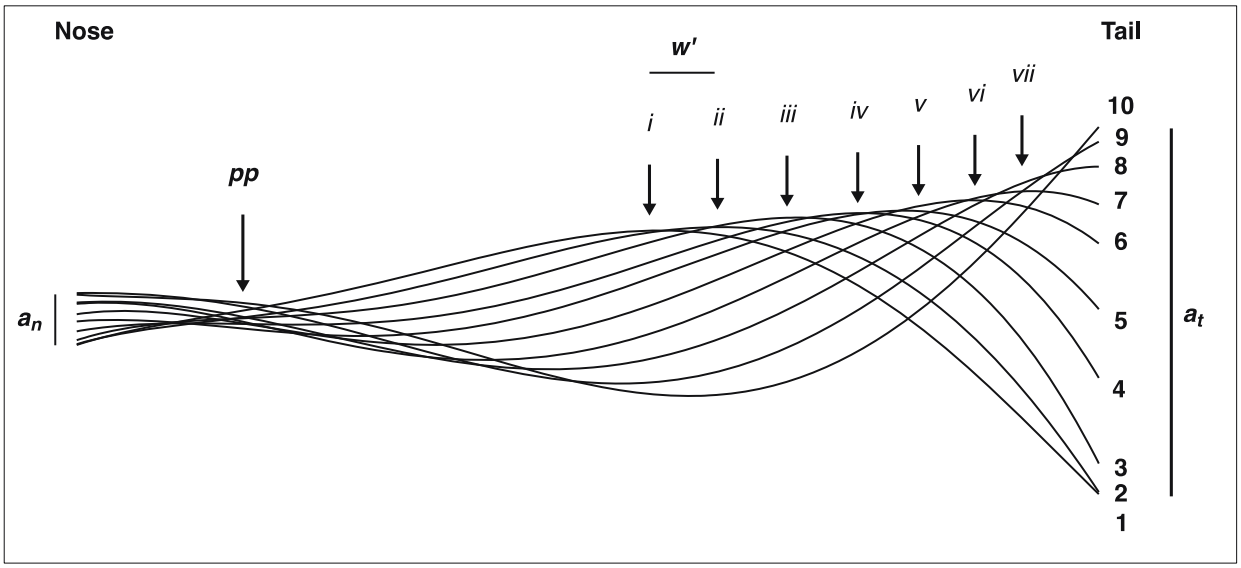

Fig. S1.

Midline analysis of ram and beat-glide swimming in *Engraulis mordax*.

After Shadwick and Gemballa (2006). This shows how midline data was analyzed. Lines are constructed midlines (see Methods) over a half stroke cycle from left-most (#1) to right-most (#10) tail extents (not all are shown). Roman numerals *i* – *vii* show the most lateral point of the body for the corresponding number midline (1 – 7). The distances between these (***w'***) were used to calculate the velocity of the propulsive wave (***w***). ***pp*** is the pivot point, the region of least lateral movement; a_t is the amplitude at the tail; a_n is the amplitude at the nose.

Table S1. Summary of Pearson correlations to assess pairwise linear dependence between measured parameters as in Fig. 4. Significantly correlations within each swimming mode are highlighted in **bold**, and those which are significant in both swimming modes are additionally **underlined**. ***A***, amplitude (***L***); ***θ***, yaw angle (°); ***U***, speed (L s^{-1}); ***F***, tailbeat frequency (str s^{-1}); ***Ds***, distance covered per stroke (***L*** str^{-1}). See Fig. 3 for plots of each relationship.

		Ram filter feeding		
	A	***θ***	***U***	***F***
θ	**r = 0.72, P = 0.01**			
U	r = 0.37, P = 0.24	r = 0.00, P = 1.00		
F	r = -0.44, P = 0.15	r = -0.40, P = 0.20	r = 0.37, P = 0.23	
Ds	**r = 0.76, P = 0.004**	r = 0.38, P = 0.22	**r = 0.67, P = 0.02**	r = -0.42, P = 0.18
		Beat-glide swimming		
	A	***θ***	***U***	***F***
θ	r = 0.09, P = 0.79			
U	r = 0.46, P = 0.13	r = 0.13, P = 0.70		
F	r = 0.22, P = 0.48	r = 0.22, P = 0.49	**r = 0.73, P = 0.01**	
Ds	**r = 0.83, P = 0.003**	r = 0.40, P = 0.25	r = 0.32, P = 0.36	r = 0.27, P = 0.45

Table S2. Depth calculations

Click here to Download Table S2